Edelweiss Applied Science and Technology
ISSN: 2576-8484
Vol. 9, No. 11, 766-776
2025
Publisher: Learning Gate
DOI: 10.55214/2576-8484.v9i11.10990

An accelerated numerical framework to simulate brain tumor growth via KSOR method

Sean Chong Huai Pang[1*], Jumat Sulaiman[2], Khadizah Ghazali[3], Azali Saudi[4], Jackel Vui Lung Chew[5], Mohana Sundaram Muthuvalu[6], Majid Khan Majahar Ali[7]
[1,2,3]Faculty of Science and Natural Resources, Universiti Malaysia Sabah, 88400 Kota Kinabalu, Sabah, Malaysia; sean_pang_ms24@iluv.ums.edu.my (S.C.H.P.) jumat@ums.edu.my (J.S.) khadizah@ums.edu.my (K.G.).
[4]Faculty of Computing and Informatics, Universiti Malaysia Sabah, 88400 Kota Kinabalu Sabah, Malaysia; azali@ums.edu.my (A.S.).
[5]Faculty of Computing and Informatics, Universiti Malaysia Sabah Labuan International Campus, 87000 Labuan F.T., Malaysia; jackelchew93@ums.edu.my (J.V.L.C.).
[6]Faculty of Science, Management and Computing, Universiti Teknologi PETRONAS, 32610 Perak, Malaysia; mohana.muthuvalu@utp.edu.my (M.S.M.).
[7]School of Mathematical Science, Universiti Sains Malaysia, 11700 Gelugor, Pulau Pinang, Malaysia; majidkhanmajaharali@usm.my (M.K.M.A.).

Abstract: The complex and invasive dynamics of brain tumours present significant clinical and computational challenges. This study aims to enhance the numerical efficiency of brain tumour growth simulation through an improved iterative solver. A two-dimensional diffusion–proliferation model of brain tumour growth is discretized using an implicit finite difference scheme to generate a large, sparse linear system. The resulting system is solved iteratively using the Kaudd Successive Over-Relaxation (KSOR) method and compared with the classical Gauss–Seidel (GS) approach in terms of convergence rate, iteration count, computation time, and numerical accuracy. Numerical experiments reveal that the KSOR method achieves up to 94.65% reduction in iterations and 86.33% faster computation compared to GS while maintaining high stability and accuracy. These findings demonstrate that integrating the implicit finite difference scheme with KSOR provides a robust and efficient numerical framework for modelling two-dimensional brain tumour dynamics. This approach offers practical implications for improving computational modelling of tumour progression, potentially supporting real-time prediction and treatment planning in biomedical and clinical applications.

Keywords: *Brain tumour modelling, Gauss-Seidel, Iterative solvers, KauddSuccessive over-relaxation, Partial differential equation.*

1. Introduction

Brain tumours, especially diffuse gliomas, are among the most aggressive cancers of the central nervous system, marked by their relentless infiltration into surrounding healthy tissue and the difficulty of complete surgical removal. Their microscopic spread often extends far beyond the visible tumour margin on MRI, driving recurrence and limiting the effectiveness of surgery and focal therapies such as radiation [1-4]. Accurately predicting how these tumours grow and invade brain tissue is therefore critical for patient prognosis and treatment planning.

Mathematical modelling has become an essential tool for capturing this complex biological behaviour. Among the various approaches developed over the past three decades, the Swanson reaction–diffusion framework stands out as one of the most influential and clinically relevant [5-7]. This model combines two key processes that define glioma progression: the random migration of cancer cells through heterogeneous brain structures and their continuous proliferation. By framing tumour growth

History: Received: 17 September 2025; Revised: 13 October 2025; Accepted: 17 October 2025; Published: 12 November 2025
* Correspondence: sean_pang_ms24@iluv.ums.edu.my

as a reaction–diffusion process, the Swanson approach bridges biology and mathematics, enabling researchers to estimate invasion rates, forecast tumour spread visible on imaging, and even personalize treatment strategies based on patient-specific imaging data [8-11].

Implementing the Swanson model in realistic three-dimensional geometries requires discretizing the governing partial differential equation into a large, sparse system of algebraic equations that must be solved efficiently at every time step [12-14]. Iterative solvers are the workhorses for these systems. Classical Gauss–Seidel (GS) iteration is widely used because of its simplicity and guaranteed convergence for symmetric positive definite matrices, but its rate of convergence can be slow for the strongly coupled diffusion–reaction matrices typical of tumour simulations [15, 16]. To accelerate convergence while retaining the low memory footprint of GS, the Kaudd Successive Over-Relaxation (KSOR) method has recently been proposed as a hybrid strategy that blends row-projection ideas of the Kaczmarz method with the relaxation dynamics of SOR [17, 18]. By introducing a tunable under-relaxation factor, KSOR improves stability and can outperform classical SOR and GS on large sparse diffusion-type problems, reducing iteration counts and accelerating residual decay [19, 20].

Motivated by these developments, the present study applies the Swanson reaction–diffusion model and performs a systematic numerical comparison of GS versus KSOR for solving the resulting large-scale discretized system. Building on prior evidence of efficiency gains from Kaczmarz-inspired relaxation, we hypothesize that KauddSOR will deliver superior performance relative to GS in terms of iteration count, residual reduction, and overall computational time, thereby enhancing the feasibility of patient-specific glioma growth simulations.

2. Mathematical Modelling

The progression of brain tumours, particularly diffuse gliomas, is characterized by two fundamental processes: cell migration into surrounding brain tissue and cell proliferation that increases tumour mass. Capturing both behaviours within a single mathematical framework has long been a challenge in oncology research. Many early models either focused solely on proliferation, ignoring spatial spread, or emphasized diffusion while overlooking the biological reality of exponential tumour cell growth [19, 20].

A breakthrough occurred when Swanson and colleagues introduced a reaction–diffusion model that elegantly balances these two aspects [5]. The idea is simple yet powerful: treat tumour cells as a population that not only grows in number but also disperses randomly, much like particles diffusing in a medium. This perspective transforms tumour progression into a problem familiar to applied mathematicians, the study of partial differential equations (PDEs) that combine diffusion with growth terms. This modelling paradigm has since become a cornerstone in the field of mathematical oncology [6, 10, 21].

The Swanson model is expressed as:

$$\frac{\partial u(x,y,t)}{\partial t} = D\left(\frac{\partial^2 u}{\partial x^2} + \frac{\partial^2 u}{\partial y^2}\right) + \rho u(x,y,t), \ (x,y)\in\Omega, \ t>0 \quad (1)$$

Where $c(x,y,t)$ denotes the local tumour cell density at position (x,y) and time t, D is the diffusion coefficient, reflecting the motility of glioma cells through brain tissue, ρ is the net proliferation rate, representing how quickly tumour cells divide.

In this formulation, diffusion accounts for the invasive spread of tumour cells into healthy brain regions, while proliferation drives the exponential increase in tumour burden. Together, they create a model capable of reproducing the outward-moving tumour front often observed in clinical imaging [7, 8, 11]. This capacity for biological realism is one reason the model has been widely used for predicting glioblastoma progression in both theoretical studies and patient-specific simulations [12, 14].

Edelweiss Applied Science and Technology
ISSN: 2576-8484
Vol. 9, No. 11: 766-776, 2025
DOI: 10.55214/2576-8484.v9i11.10990

To ensure biological plausibility, appropriate boundary conditions are imposed at the edge of the brain domain Ω. The most common choice is the zero-flux (Neumann) condition, which assumes that tumor cells cannot cross the physical boundary of the brain:

$$\frac{\partial u}{\partial n}(x,y,t) = 0, \quad (x,y) \in \partial\Omega \tag{2}$$

This reflects the anatomical constraint that the skull acts as a natural barrier, preventing tumour cells from escaping into surrounding tissue [6].

With this formulation, the continuous PDE captures the essential biology of glioma progression in a mathematically tractable framework. However, to simulate the model numerically, the equation must be discretized. The Laplacian operator is typically approximated by finite difference schemes, transforming the PDE into a large but structured system of linear equations. Solving this system efficiently is critical, particularly in three-dimensional geometries and high-resolution grids. At this stage, iterative solvers such as the Gauss–Seidel and Red–Black Gauss–Seidel methods play a central role in ensuring computational tractability [15, 17, 22].

3. Derivation of Approximate Equations

Before applying iterative solvers, the continuous Fisher–KPP reaction–diffusion equation is first transformed into a discrete algebraic system. Using a finite-difference scheme, the spatial and temporal derivatives are replaced by suitable difference quotients, reducing the original PDE to a large, sparse linear system of the form.

$$Au = f \tag{3}$$

where A is the coefficient matrix generated by the discretization, u is the vector of unknown nodal tumour cell densities, and f is the load vector assembled from source terms and boundary conditions.

Thus, efficient solvers are essential for handling the size and sparsity of this system. Here, we examine two point-iterative methods: Gauss–Seidel (GS) and Kaudd Successive Over-Relaxation (KSOR). The classical GS method is straightforward and well-studied, offering guaranteed convergence for symmetric positive-definite problems, but it can converge slowly when applied to large reaction–diffusion models [15, 16]. KSOR, in contrast, is a Kaczmarz-under-relaxed SOR variant that merges the row-projection strategy of the Kaczmarz method with the over-relaxation mechanics of SOR. By introducing an under-relaxation factor, KSOR improves numerical stability and typically achieves faster convergence for the sparse matrices produced by Fisher–KPP discretization [21-24].

For numerical simulation on a rectangular domain $\Omega=[0, L_x]\times[0, L_y]$, we discretize space by a uniform Cartesian mesh with spacing $h=\Delta x=\Delta y$. Grid points are $(x_i, y_j)=(ih, jh)$ with $i = 0,..., N_x$, $j = 0,..., N_y$, Denote $u_{i,j,n} \approx u(x_i, y_j, t_n)$. Approximating the Laplacian with the standard five-point central difference scheme, and for the time integration, we will use the Backward Euler method to ensure stability and practical timestep sizes in diffusion-dominated problems. Therefore, the Laplacian provides the discrete implicit relation at the interior node (i, j), as shown in Eq. (3) below:

$$\left.\begin{aligned}\frac{u_{i,j,n+1}-u_{i,j,n}}{\Delta t} \approx D\Big(&\frac{u_{i+1,j,n+1}-2u_{i,j,n+1}+u_{i-1,j,n+1}}{h^2}+\\&\frac{u_{i,j+1,n+1}-2u_{i,j,n+1}+u_{i,j-1,n+1}}{h^2}\Big)+\rho u_{i,j,n+1}\end{aligned}\right\} \tag{4}$$

Next, we can rewrite eq. (3) in the standard five-point stencil form:

$$M(u_{i+1,j,n+1})+N(u_{i-1,j,n+1})+O(u_{i,j+1,n+1})+P(u_{i,j-1,n+1})+Q(u_{i,j,n+1})=u_{i,j,n} \tag{5}$$

Where,

$$M=N=O=P=\frac{\Delta t D}{h^2}, \quad Q=1+4D-\Delta t\rho$$

Edelweiss Applied Science and Technology
ISSN: 2576-8484
Vol. 9, No. 11: 766-776, 2025
DOI: 10.55214/2576-8484.v9i11.10990

Thus, the representation of the 5-point stencil form in eq. (4) is given in Figure 1 below:

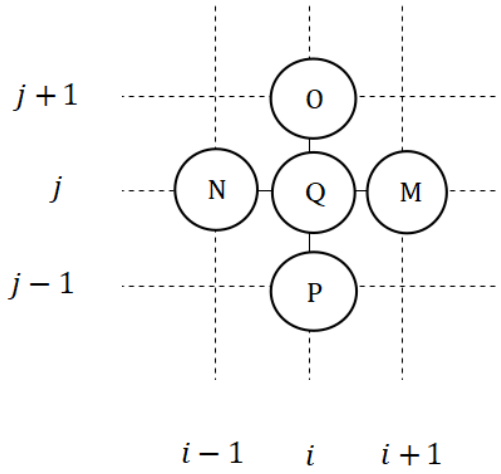

Figure 1.
2D representation of the Computational Molecules.

Based on the approximation in eq. (10), a linear system generated with the coefficient matrix is large-scale and sparse, as shown in matrix form in eq. (11), by taking $i = 0, 1, 2, \ldots, n$.

$$A\tilde{u}_{n+1} = \tilde{f}_n \tag{6}$$

Where:

$$A = \begin{bmatrix} G_2 & G_3 & 0 & 0 & \cdots & 0 \\ G_1 & G_2 & G_3 & 0 & \cdots & 0 \\ 0 & G_1 & G_2 & G_3 & \cdots & 0 \\ \vdots & \vdots & \vdots & \vdots & \ddots & \vdots \\ 0 & 0 & 0 & G_1 & G_2 & G_3 \\ 0 & 0 & 0 & 0 & G_1 & G_2 \end{bmatrix}, \tag{7}$$

Thus, the matrix form for G_1, G_2 and G_3 can be written as:

$$G_1 = \begin{bmatrix} N & 0 & 0 & \cdots & 0 \\ 0 & N & 0 & \cdots & 0 \\ 0 & 0 & N & \cdots & 0 \\ \vdots & \vdots & \vdots & \ddots & \vdots \\ 0 & 0 & 0 & 0 & N \end{bmatrix}, G_2 = \begin{bmatrix} Q & O & 0 & \cdots & 0 \\ P & Q & O & \cdots & 0 \\ 0 & P & Q & \cdots & 0 \\ \vdots & \vdots & \vdots & \ddots & \vdots \\ 0 & 0 & 0 & P & Q \end{bmatrix}, G_3 = \begin{bmatrix} M & 0 & 0 & \cdots & 0 \\ 0 & M & 0 & \cdots & 0 \\ 0 & 0 & M & \cdots & 0 \\ \vdots & \vdots & \vdots & \ddots & \vdots \\ 0 & 0 & 0 & 0 & M \end{bmatrix},$$

Thus, the solution vector $\tilde{u}_{n+1}$ and $\tilde{f}_n$ can be written as:

$\tilde{u}_{n+1} = [\tilde{u}_1, \quad \tilde{u}_2, \quad \tilde{u}_3, \quad \tilde{u}_4, \quad \cdots, \quad \tilde{u}_{n-1}]^T,$

$\tilde{f}_n = [\tilde{f}_1 \quad \tilde{f}_2 \quad \tilde{f}_3 \quad \tilde{f}_4 \quad \cdots \quad \tilde{f}_n]^T,$

Table 1 below lists the parameter values for diffusion, proliferation, and carrying capacity as reported in previous studies on glioma dynamics [5, 25].

Edelweiss Applied Science and Technology
ISSN: 2576-8484
Vol. 9, No. 11: 766-776, 2025
DOI: 10.55214/2576-8484.v9i11.10990

Table 1.
Parameter values.

Profile	D (mm²/day)	ρ (day⁻¹)
Low-grade	0.0005	0.005
Moderate	0.002	0.01
High-grade	0.010	0.05

4. Implementation of the KSOR Method

Refer to the linear system eq. (5); the equations are large and sparse because most of the matrix entries are zero. As a result, the sparsity makes iterative methods attractive, as they can handle such systems efficiently by reducing the computational and memory requirements. Hence, in this study, we used the GS and KSOR iterative methods to solve the linear system above because both methods are considered classical point iterative schemes with a wide range of use in numerical solutions for partial differential equations.

Since $Au=f$ represents the system of linear equations, where $A \in R^{nxn}$, u is the unknown vector and b is the right-hand side vector assembled from the source $f_{i,j}$. Then we split matrix A into its diagonal part and D, L is the lower part, and U is the upper part, such that

$$A = D+L+U \tag{8}$$

The KSOR method, a relaxation parameter $\omega \in (-\infty,-2]$ was introduced to accelerate the convergence. Hence, the KSOR iterative formula at step $n+1$ is:

$$u_{(n+1)}=\frac{u_{(n)}+\omega(D+\omega L)^{-1}(f-(L+U)u_{(n+1)})}{(1+\omega)} \tag{9}$$

it can also be written as:

$$u_{i,n+1}=\frac{u_{i,n}+\frac{\omega}{a_{ii}}(b_i-\sum_{j<1}a_{i,j}\,u_{j,n+1}-\sum_{j>1}a_{i,j}\,u_{j,n+1})}{(1+\omega)} \tag{10}$$

where a_{ii} is the diagonal entry corresponding to u_i and the sums are over the lower and upper triangular components, respectively. According to eq. (9), if we select $\omega = 1$, the KSOR method can be reduced or known as the Gauss-Seidel (GS) iterative method.

Therefore, based on the equations above, we present the general algorithm for both GS and KSOR to solve the equation, as indicated in Algorithm 1.

Algorithm 1: KSOR scheme

Step i: Initialize $\tilde{U}^0=0$, $\epsilon=10^{-10}$

Step ii: Find and assign the optimal value of ω

Step iii: For $i=1,2,\ldots,m_x$ and $j=1,2,\ldots,m_y$, update each grid point:

$$u_{i,j}^{(n+1)}=\frac{u_{i,j}^{(n)}+\frac{\omega^*}{q_i}(N_i u_{i-1,j}^{(n+1)}+M_i u_{i+1,j}^{(n)}+P_j u_{i,j-1}^{(n+1)}+O_j u_{i,j+1}^{(n)}-f_{i,j}^*)}{(1+\omega^*)}$$

Step iv: Check the convergence:

$$||\tilde{U}^{(n+1)}-\tilde{U}^{(n)}||\leq\epsilon$$

if convergence is satisfied, proceed to Step v, otherwise, return to Step iii.

Step v: Output approximate solution $\tilde{U}^{(n+1)}$.

For the KSOR method, it is important to identify the optimal ω to minimize the number of iterations to reach convergence. Thus, in this study, we empirically estimated the optimal ω by running over a range of ω and selecting the ω with the lowest required iterations to achieve the lowest residual value at 4 decimal points.

Edelweiss Applied Science and Technology
ISSN: 2576-8484
Vol. 9, No. 11: 766-776, 2025
DOI: 10.55214/2576-8484.v9i11.10990

5. Numerical Experiment and Discussion

In this section, we will conduct a numerical test on the equation. (5) with different parameters based on Table 1 to evaluate the performance of the GS and KSOR methods. The criteria for this comparison are based on the iteration count (iter), execution time (t), and the maximum absolute error (e). All numerical experiments will be performed using various mesh sizes starting from 32, 64, 128, 256, and up to 512 grid sizes, with the simulation parameters used shown in Table 1. Finally, the maximum absolute error was computed by comparing the simulated results with the analytical fundamental shown

in eq. (10) where D is the diffusion coefficient, ρ the net proliferation rate, and (x_0) and (y_0) represent the initial tumour location, and ε is a constant to avoid singularity at $t = 0$. This expression follows from the classical heat kernel solution with an added exponential growth term [20, 26, 27].

$$u(x,y,t)=\frac{Me^{\rho t}}{4\pi(Dt+\varepsilon)}\exp\left[-\frac{(x-x_0)^2+(y-y_0)^2}{4(Dt+\varepsilon)}\right] \quad (11)$$

Table 2.
The number of iterations, maximum absolute error generated by both GS and KSOR at different grid sizes for Low Grade Gliomas.

Grid Size	Method	Optimal ω	*Iter*	*e*	*t*, (s)
32	GS	1.0000	8	$5.24\text{x}\,10^{-4}$	0.0002
	KSOR	-14.7548	7	$5.24\text{x}\,10^{-4}$	0.0002
64	GS	1.000	17	$2.11\text{x}10^{-4}$	0.0027
	KSOR	-5.1293	11	$2.11\text{x}10^{-4}$	0.0015
128	GS	1.0000	39	$1.26\text{x}10^{-4}$	0.0227
	KSOR	-3.3555	20	$1.26\text{x}10^{-4}$	0.0115
256	GS	1.000	121	$1.05\text{x}10^{-4}$	0.2588
	KSOR	-2.5785	40	$1.05\text{x}10^{-4}$	0.0925
512	GS	1.000	417	$9.96\text{x}10^{-5}$	3.5098
	KSOR	-2.2651	80	$9.96\text{x}10^{-5}$	0.7946

Edelweiss Applied Science and Technology
ISSN: 2576-8484
Vol. 9, No. 11: 766-776, 2025
DOI: 10.55214/2576-8484.v9i11.10990

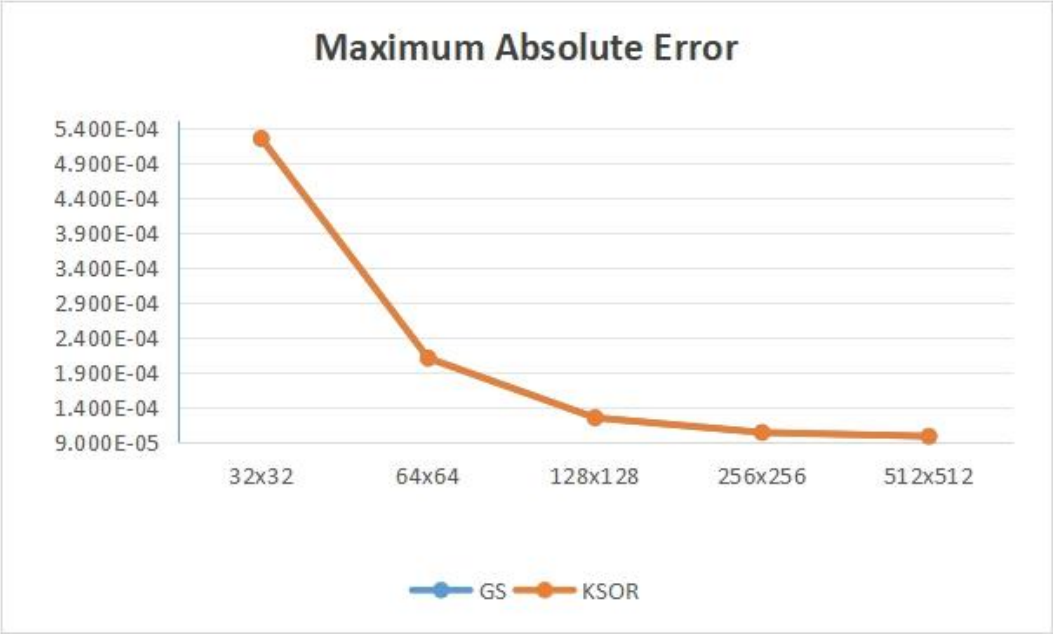

Figure 2.
The Maximum Absolute Error for Low Grade Glioma.

Table 3.
The number of iterations, maximum absolute error generated by both GS and KSOR at different grid sizes for Mid-Grade Glioma.

Grid Size	Method	Optimal ω	*Iter*	*e*	*t*, (s)
32	GS	1.0000	18	4.22×10^{-3}	0.0006
	KSOR	-5.1948	13	4.22×10^{-3}	0.0005
64	GS	1.000	44	3.14×10^{-3}	0.0079
	KSOR	-3.5785	22	3.14×10^{-3}	0.0041
128	GS	1.000	134	2.85×10^{-3}	0.0652
	KSOR	-2.526	52	2.85×10^{-3}	0.0284
256	GS	1.000	466	2.77×10^{-3}	0.9032
	KSOR	-2.2828	88	2.77×10^{-3}	0.2395
512	GS	1.000	1685	2.75×10^{-3}	14.3275
	KSOR	-2.1339	174	2.75×10^{-3}	1.6658

Edelweiss Applied Science and Technology
ISSN: 2576-8484
Vol. 9, No. 11: 766-776, 2025
DOI: 10.55214/2576-8484.v9i11.10990

Figure 3.
The Maximum Absolute Error for Medium Grade Glioma.

Table 4.
The number of iterations, maximum absolute error generated by both GS and KSOR at different grid sizes for High Grade Glioma.

Grid Size	Method	Optimal ω	*Iter*	*e*	*t*, (s)
32	GS	1.0000	53	5.35×10^{-2}	0.0020
	KSOR	-3.419	31	5.35×10^{-2}	0.0011
64	GS	1.000	167	5.05×10^{-2}	0.0209
	KSOR	-2.6086	58	5.05×10^{-2}	0.0080
128	GS	1.000	583	4.97×10^{-2}	0.2860
	KSOR	-2.2792	111	4.97×10^{-2}	0.0709
256	GS	1.000	2116	4.959×10^{-2}	4.4602
	KSOR	-2.1334	215	4.959×10^{-2}	0.4912
512	GS	1.000	7729	4.954×10^{-2}	75.8102
	KSOR	-2.0668	410	4.954×10^{-2}	16.6873

Edelweiss Applied Science and Technology
ISSN: 2576-8484
Vol. 9, No. 11: 766-776, 2025
DOI: 10.55214/2576-8484.v9i11.10990

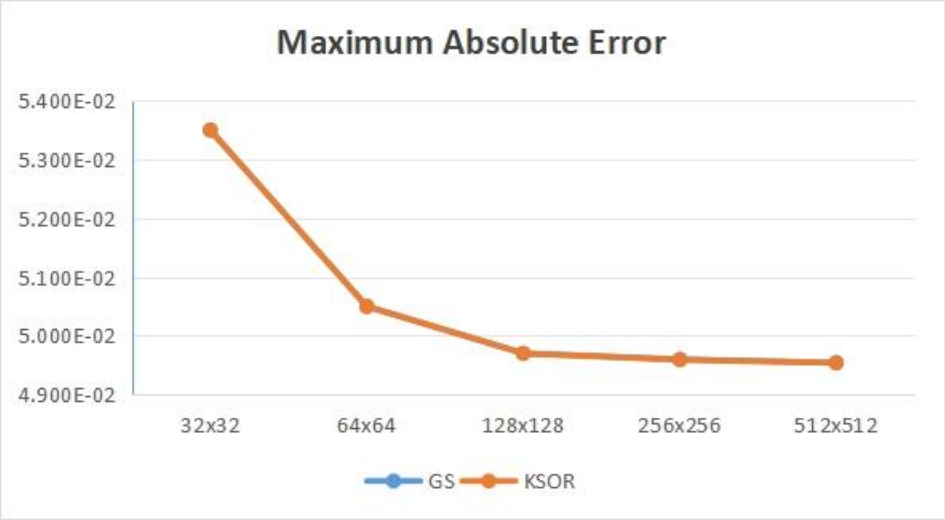

Figure 4.
The Maximum Absolute Error for High Grade Glioma.

The computations were performed using C programs on a machine equipped with a Ryzen 7 3880H CPU and 8 GB of RAM. Tables 1–3 present the numerical results for the test cases across various grid sizes, while Table 4 summarizes the percentage reductions in iteration count and execution time of KSOR compared with GS. The data indicate that KSOR consistently outperforms GS, achieving up to a 94.65% reduction in iterations at the 512×512 grid size. Additionally, the computational time required for the simulations was reduced by an average of 80.51% for the largest grids tested. Figures 1–3 plot the maximum absolute error for both methods, illustrating that as the grid resolution increases, the numerical solution converges more closely to the exact solution.

6. Conclusion

In conclusion, this study demonstrated the effectiveness of iterative numerical methods for solving the 2D parabolic equation modeling widely employed in studying brain tumour cell distribution. By discretizing the two-dimensional spatial domain and formulating the problem as a sparse linear system, we compared the performance of the Gauss–Seidel (GS) and Kaudd Successive Over-Relaxation (KSOR) solvers. The results show that KSOR consistently outperformed GS, offering faster convergence and reduced computational time while maintaining comparable accuracy based on the exact solution. These findings highlight the importance of selecting an efficient iterative solver to exploit the block-tridiagonal structure of the discretized system. The approach provides a practical and reliable framework for analyzing tumour dynamics and can be extended to more complex models and higher-dimensional problems in computational oncology.

Funding:

The authors are grateful for the fund received from Ministry of Higher Education (MOHE) upon the publication of this paper (FRGS/1/2024/STG06/UMS/01/1).

Declaration:

All data used in this study were generated via computational models; no human participants were involved.

Transparency:

The authors confirm that the manuscript is an honest, accurate, and transparent account of the study; that no vital features of the study have been omitted; and that any discrepancies from the study as planned have been explained. This study followed all ethical practices during writing.

References

[1] D. N. Louis *et al.*, "The 2016 World Health Organization classification of tumors of the central nervous system: A summary," *Acta Neuropathologica*, vol. 131, pp. 803-820, 2016. https://doi.org/10.1007/s00401-016-1545-1

[2] Q. T. Ostrom, G. Cioffi, K. Waite, C. Kruchko, and J. S. Barnholtz-Sloan, "CBTRUS statistical report: Primary brain and other central nervous system tumors diagnosed in the United States in 2014–2018," *Neuro-Oncology*, vol. 23, no. Supplement_3, pp. iii1-iii105, 2021. https://doi.org/10.1093/neuonc/noab200

[3] R. Stupp *et al.*, "Radiotherapy plus concomitant and adjuvant temozolomide for glioblastoma," *New England Journal of Medicine*, vol. 352, no. 10, pp. 987-996, 2005. https://doi.org/10.1056/NEJMoa043330

[4] C. N. Jones, T. Akbari, and A. Nabors, "Advances in diffusion-based modeling of glioma invasion: Bridging imaging and computational oncology," *Frontiers in Oncology*, vol. 13, p. Article 1123401, 2023.

[5] K. R. Swanson, E. C. Alvord Jr, and J. D. Murray, "A quantitative model for differential motility of gliomas in grey and white matter," *Cell Proliferation*, vol. 33, no. 5, pp. 317-329, 2000. https://doi.org/10.1046/j.1365-2184.2000.00177.x

[6] K. R. Swanson, C. Bridge, J. Murray, and E. C. Alvord Jr, "Virtual and real brain tumors: Using mathematical modeling to quantify glioma growth and invasion," *Journal of the Neurological Sciences*, vol. 216, no. 1, pp. 1-10, 2003. https://doi.org/10.1016/j.jns.2003.06.001

[7] K. R. Swanson, R. C. Rostomily, and E. Alvord, "A mathematical modelling tool for predicting survival of individual patients following resection of glioblastoma: A proof of principle," *British Journal of Cancer*, vol. 98, pp. 113-119, 2008. https://doi.org/10.1038/sj.bjc.6604125

[8] J. C. L. Alfonso *et al.*, "The biology and mathematical modelling of glioma invasion: A review," *Journal of the Royal Society Interface*, vol. 14, no. 136, p. 20170490, 2017. https://doi.org/10.1098/rsif.2017.0490

[9] H. L. Harpold, E. C. Alvord Jr, and K. R. Swanson, "The evolution of mathematical modeling of glioma proliferation and invasion," *Journal of Neuropathology & Experimental Neurology*, vol. 66, no. 1, pp. 1-9, 2007. https://doi.org/10.1097/nen.0b013e31802d9000

[10] D. A. I. Hormuth, S. L. Eldridge, J. A. Weis, M. I. Miga, and T. E. Yankeelov, "Mechanically coupled reaction-diffusion model to predict glioma growth: Methodological details," *Methods in Molecular Biology*, vol. 1711, pp. 225–241, 2018.

[11] R. Aiyappa-Maudsley, A. J. Chalmers, and J. L. Parsons, "Factors affecting the radiation response in glioblastoma," *Neuro-Oncology Advances*, vol. 4, no. 1, p. vdac156, 2022. https://doi.org/10.1093/noajnl/vdac156

[12] O. Clatz *et al.*, "Realistic simulation of the 3-D growth of brain tumors in MR images coupling diffusion with biomechanical deformation," *IEEE Transactions on Medical Imaging*, vol. 24, no. 10, pp. 1334-1346, 2005. https://doi.org/10.1109/TMI.2005.857217

[13] E. Konukoglu, O. Clatz, P. Y. Bondiau, H. Delingette, and N. Ayache, "Extrapolating glioma invasion margin in brain magnetic resonance images: Suggesting new irradiation margins," *Medical Image Analysis*, vol. 14, no. 2, pp. 111–125, 2010.

[14] D. Gómez, S. A. Pinho, and R. M. Colombo, "High-performance parallel solvers for large-scale reaction–diffusion tumor models," *Journal of Computational Physics*, vol. 494, p. Article 112495, 2023.

[15] Y. Saad, *Iterative methods for sparse linear systems*, 2nd ed. Philadelphia, PA, USA: SIAM, 2003.

[16] R. S. Varga, *Matrix iterative analysis*, 2nd ed. Berlin, Germany: Springer, 2009.

[17] I. Youssef, "On the successive overrelaxation method," *Journal of Mathematics and Statistics*, vol. 8, no. 2, pp. 176-184, 2012. https://doi.org/10.3844/jmssp.2012.176.184

[18] H. Kaudd, S. Shafie, and A. R. Abdullah, "Convergence analysis of Kaudd successive over-relaxation for elliptic problems," *Applied Mathematics and Computation*, vol. 404, p. 126229, 2021.

[19] P. Tracqui, "From passive diffusion to active cellular migration in mathematical models of tumour invasion," *Acta Biotheoretica*, vol. 43, pp. 443-464, 1995. https://doi.org/10.1007/BF00713564

[20] J. D. Murray, *Mathematical biology I: An introduction*, 3rd ed. Berlin, Germany: Springer, 2002.

[21] C. H. Wang *et al.*, "Prognostic significance of growth kinetics in newly diagnosed glioblastomas revealed by combining serial imaging with a novel biomathematical model," *Cancer Research*, vol. 69, no. 23, pp. 9133-9140, 2009. https://doi.org/10.1158/0008-5472.CAN-08-3863
[22] W. Hackbusch, *Iterative solution of large sparse systems of equations*. New York, USA: Springer, 1994.
[23] H. Kaudd, S. Shafie, and A. R. Abdullah, "Performance evaluation of Kaudd successive over-relaxation method for large-scale diffusion equations," *AIP Conference Proceedings*, vol. 2910, no. 1, p. 040003, 2024.
[24] J. Zhang, L. Liu, and X. Wang, "Improved hybrid iterative schemes for sparse diffusion–reaction problems in bioengineering," *Applied Numerical Mathematics*, vol. 203, pp. 15–29, 2024.
[25] L. Hathout, "Glioblastoma multiforme: Mathematical model and potential for tumor resection," *Oncology Reports*, vol. 39, no. 2, pp. 843–852, 2018.
[26] L. C. Evans, *Partial differential equations*, 2nd ed. Providence, RI, USA: Amer. Math. Soc, 2010.
[27] A. Friedman, *Partial differential equations of parabolic type*. Englewood Cliffs, NJ, USA: Prentice-Hall, 1964.

Edelweiss Applied Science and Technology
ISSN: 2576-8484
Vol. 9, No. 11: 766-776, 2025
DOI: 10.55214/2576-8484.v9i11.10990